Journal of Engineering Science and Technology
Vol. 13, No. 10 (2018) 3092 - 3115

ANCILLARY SERVICE REQUIREMENT BASED AUTOMATIC GENERATION CONTROL ASSESSMENT IN A DEREGULATED POWER SYSTEM WITH HES AND IPFC UNITS

B. BASKAR[1,*], B. PARAMASIVAM[2], I. A. CHIDAMBARAM[3]

[1]Department of EEE, Government Polytechnic College, Sankarapuram, Tamilnadu, India
[2]Department of EEE, Government College of Engineering, Bodinayakkanur, Tamilnadu India
[3]Department of Electrical Engineering, Annamalai University, Annamalainagar, Tamilnadu, India
*Corresponding Author: baskar.prb@gmail.com

Abstract

This paper intends the evaluation measures for obtaining the Ancillary ServicesRequirement (ASR) indices stand on Automatic Generation Control (AGC) in a deregulated power system.Ancillary services are vital to support the transmission of electric power from vendor to user with the responsibility of control areas and transmitting utilities within those control areas to maintain steadfast operations of the interconnected power system under deregulated environment. In this swot, Proportional Integral Derivative with derivative Filter (PIDF) is projected for the AGC loop of a two-area thermal power system with reheat bicycle mix condensation turbine. The control constraints of the PIDF controller are optimized using the Big Bang Big Crunch (BBBC) algorithm.ASR keys are computed stranded on the dynamic response of the control input deviations and the mechanical power generation deviations of each area for dissimilar nature of possible transactions. These indices designate the ancillary service requirements and are required to improve the competence of the physical operation of the power system with the augmented transmission capacity in the network. An advanced application of Hydrogen Energy Storage (HES), when coordinated with the Interline Power Flow Controller (IPFC) for the development of AGC loop of a two-area thermal power system is also painstaking. Simulation reveals that the proposed PIDF controller tuned with BBBC algorithm perk up the dynamic output response of the test system. Moreover, it can also be pragmatic that the ASR Indices are computed for a two-area thermal power system with HES and IPFC units indicates that the new advanced control for a better restoration of the power system output responses and ensure enhanced ASR indices in order to afford the superior margin of steadiness.

Keywords: AGC, ASR indices, BBBC algorithm, HES, IPFC, PIDF controller.

1. Introduction

In a deregulated power bazaar, apart from the firm transaction of the energy and power, Independent System Operator (ISO) makes an agreement for certain additional services to maintain the consistency and eminence of the power supply. Ancillary services play a fundamental role in preserving an active and reactive power balance, the disparity in frequency and voltage within permissible restrictions in event of emergency handling of power system [1]. The frequency related ancillary services such as AGC system adjusts the generator set point by changing speed changer settings automatically to pay off the mismatch between total generation and total load demand plus linked system losses [2]. The objective of AGC in an interconnected power system is to minimize the fleeting deviations in area frequency, tie-line power interchange and to ensure their steady state error becomes zero [3]. The AGC action is directed by the Area Control Error (ACE), which is a function of system frequency, and tie line flows. As the ACE is focused to zero by the AGC both frequency and tie-line power errors will be put on to zero [4]. A deregulated power system comprises of generation companies (Gencos), distribution companies (Discos), transmission companies (Transco) and ISO. An ISO is a self-governing agent that manages all the transactions believed between Discos and Gencos. A Disco participation matrix (DPM) is used for a hallucination of bonds between Gencos and Discos [5]. An ISO has to perform various ancillary services for winning operation of the power system [6].

Several superior control arrangements and techniques have been proposed in literature survey for a better enhancement of AGC [7-10]. However, these superior approaches are found to be complex in nature and have to ease with the users in adopting these techniques thus reducing their applicability. Alternatively, the performances a classical controller such as Integral *(I),* Proportional Integral *(*PI*),* Integral Derivative *(*ID*)* and Proportional Integral Derivative (PID) controller are practically the same from the viewpoint of dynamic responses. In a PID controller, the derivative mode improves the stability of the system and increases the speed of the controller response but it makes the plant to draw a huge amount of control input. Also, any noise in the control input signal will result in large plant input signals distortion, which often leads to complications in practical applications. The practical solution to these problems is to put the first filter on the imitative term and tune its pole so that the go on due to the noise does not occur since it eases high frequency noise [11]. In this study, a Proportional Integral Derivative with derivative Filter (PIDF) controllers are intended and realized for the AGC under deregulated atmosphere problems.

Many looms such as Particle Swarm Optimization (PSO), Genetic Algorithm KHA (GA), Biogeography Based Optimization (BBO), Krill Herd Algorithm (KHA), Teaching Learning Based Optimization (TLBO) and Bacterial Foraging Optimization (BFO) algorithm have been planned to resolve the control parameters of a several standard controllers to solve the AGC problem. A wide range of control approaches along with their compensation and boundaries is given in [12]. Big Bang Big Crunch (BBBC) is an optimization based on the big bang theory and big crunch theory [13, 14]. This paper offers the determination of minimum values of the constraint of a PIDF controller for an AGC loop of a two-area thermal power system with reheat bicycle mix condensation turbine in a deregulated location using the BBBC algorithm. The minimization of an Integral square of ACE is taken as an objective function.

Balancing of power supply and demand is always an intricate procedure particularly at tip load conditions. As a result, there may be grim alarm about the reliable operation of power system. So, it is essential to include Fast-acting Energy Storage Systems (ESS) contains storage capacity in adding up with the kinetic energy of the generator rotors is wise to damp out the frequency oscillations [15, 16]. Due to the cost-effective basis, it is not promising to place EES in all the areas. Flexible AC Transmission Systems (FACTS) controllers [17] play a decisive role to control the power flow in an interconnected power system. A number of crams have explored the probable of using FACTS devices for better power system control since it offers more flexibility. When FACTS and EES units are approved in the system, allowed to act in a coordinated manner results in a better control augmentation for the network conditions in a very fast and inexpensive manner [18-20].

In this study, the concept of AGC in a two-area thermal power system having a coordinated control action with Hydrogen Energy Storage HES () and Interline Power Flow Controller (IPFC) units are proficient in controlling the network performance in a very fast manner and to improve power transfer limits for better restoration. The modern power system is pressed to significant operating limits in the market environment. The goal of power system restoration research is to discover the fast and consistent ways to restore a power system to its normal operational state after a black-out event. The idea of this paper to develop more successful and fast restoration plan using ASR index based on *AGC* assessment for a two-area thermal power system without and with HES and IPFC units in a deregulated environment. The simulation results show that the restoration process for the system with HES and IPFC units ensures enhanced ASR indices, which offer the good margin of stability.

2. Modelling of two-area thermal power system with reheat tandem Compound steam turbine in deregulated environment

In the deregulated power system, Discos in every area can bond with Gencos in its own or other areas. There are several Gencos and Discos in the deregulated power system; a Disco has the liberty to have a contract with any Genco for the contract of power. Such transactions are called bilateral transactions [5]. All the transactions have to be cleared through an impartial entity called an ISO. In this study, two-area thermal power system is considered in which each area has two Gencos and two Discos is shown in Fig. 1. The AGC performa96RK, ce is realized on the steam turbine dynamic model parameters. The steam turbine model parameters are found to be reliant on the generation schedules of thermal power plants [21]. The dynamic model of reheat bicycle mix condensation turbine is shown in Fig. 2.

The main constraints of these models are the time constants T_{SC}, T_{RH} and T_{CO} of Steam Chest (SC), Reheater (RH) and Cross-Over (CO) pipe respectively and the power fractions F_{HP}, F_{IP} and F_{LP} of High Pressure (HP), Intermediate-Pressure (IP) and Low Pressure (LP) turbines respectively. The typical values of various time constants and power portions of thermal reheat turbine can be designed for different generation schedules by removing the heat balance data is shown in *Appendix A* [21]. In the new environment, Discos may contract power from any Gencos and ISO has to supervise these contracts. DPM is a matrix in which the number of rows is equal to the number of Gencos and the number of columns is equal to the number

of Discos in the system each entry in this matrix can be considered for the portion of a total load contracted by a Disco towards a Genco. The sum of all the entries in a column DPM is unity. From the Fig. 1. Let $Genco_1$, $Genco_2$, $Disco_1$, $Disco_2$ be in area 1 and $Genco_3$, $Genco_4$, $Disco_3$, $Disco_4$ be in area 2. The corresponding DPM is given as follows

$$DPM = \begin{bmatrix} cpf_{11} & cpf_{12} & cpf_{13} & cpf_{14} \\ cpf_{21} & cpf_{22} & cpf_{23} & cpf_{24} \\ cpf_{31} & cpf_{32} & cpf_{33} & cpf_{34} \\ cpf_{41} & cpf_{42} & cpf_{43} & cpf_{44} \end{bmatrix} \quad (1)$$

where *cpf* represents "contract participation factor", i.e., *p.u*. MW load of a corresponding Disco. The scheduled steady state power flow on the tie-line is given as [5]

$$\Delta P_{Tie\ 12}^{scheduled} = \sum_{i=1}^{2}\sum_{j=3}^{4} cpf_{ij}\,\Delta P_{Lj} - \sum_{i=3}^{4}\sum_{j=1}^{2} cpf_{ij}\,\Delta P_{Lj} \quad (2)$$

The actual tie-line power is given as at dg aw3211`59\ `` 6-

$$\Delta P_{Tie\ 12}^{actual} = \frac{2\pi T_{12}}{s}(\Delta F_1 - \Delta F_2) \quad (3)$$

At any given time, the tie-line power error is given by [5]

$$\Delta P_{Tie\ 12}^{Error} = \Delta P_{Tie\ 12}^{actual} - \Delta P_{Tie\ 12}^{scheduled} \quad (4)$$

$\Delta P_{Tie\ 12}^{Error}$, vanishes in the steady as the actual tie-line power flow reaches the scheduled power flow. This error signal is used to generate the respective Area Control Error (ACE) signals as in the traditional scenario [5].

$$ACE_1 = \beta_1 \Delta F_1 + \Delta P_{Tie12}^{Error} \quad (5)$$

$$ACE_2 = \beta_2 \Delta F_2 + a_{12}\Delta P_{Tie12}^{Error} \quad (6)$$

The generation of each Genco must footpath the contracted demands of Discos in steady state. The desire total power generation of i^{th} Genco in terms of DPM entries can be calculated as

$$\Delta P_{mi} = \sum_{j=1}^{4} cpf_{ij}\,\Delta P_{Lj} \quad (7)$$

As there are two Gencos in each area, *ACE* signal has to be dispersed among them in proportion to their participation in the AGC. Coefficients that distribute ACE to Gencos are termed as "ACE Participation Factors (apfs)". In a given control area, the sum of participation factors is equal to 1. Hence, apf_{11}, apf_{12} are considered as ACE participation factor in area 1 and apf_{21}, apf_{22} are in area 2.

3. Proposed Controller and Optimization Technique

3.1. Control structure of PIDF controller

The structure of PID controller with derivative filter is shown in Fig. 3, where K_P, K_I, and K_D are the proportional, integral and derivative gains respectively and N is the derivative filter coefficient.

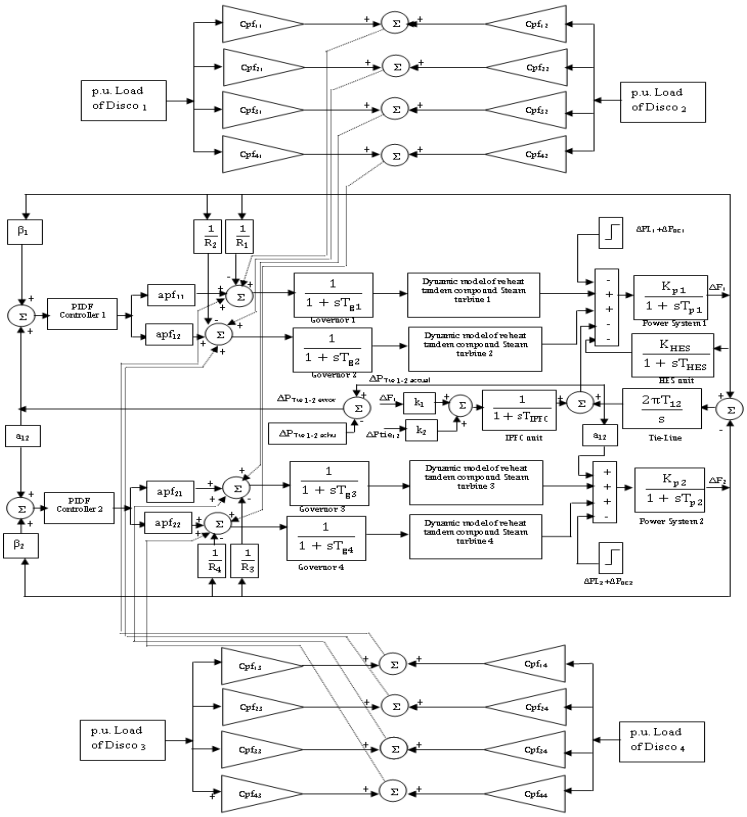

Fig. 1. Transfer function model of two area power system with HES and IPFC units in deregulated environment.

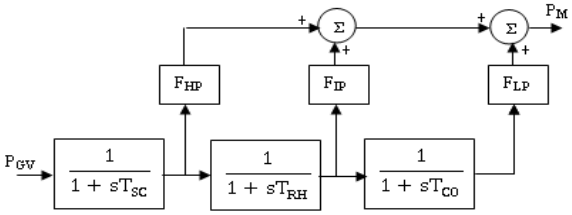

Fig. 2. Dynamic model of a reheat tandem compound steam turbine.

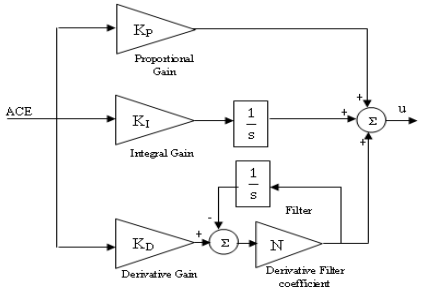

Fig. 3. Block diagram for PIDF controller.

The transfer function of proposed PIDF controller is given by

$$T(s) = K_P + \frac{K_I}{s} + K_D\left(\frac{Ns}{s+N}\right) \quad (8)$$

The *BBBC* search algorithm is used to determine the optimal constraints of *PIDF* controllers with the objective to minimize Integral Square of area control error, which can be formulated in the following manner:

$$J = \int_0^{t_{sim}} (\Delta F_1^2 + \Delta F_2^2 + \Delta P_{tie}^2)\, dt \quad (9)$$

The problem constraints are the *PIDF* controller parameter bounds. Therefore, the design problem can be formulated as,

$$Minimize J \quad (10)$$

Subject to

$$K_P^{min} \le K_P \le K_P^{max}, K_I^{min} \le K_I \le K_I^{max}, K_D^{min} \le K_D \le K_D^{max}, N^{min} \le N \le N^{max} \quad (11)$$

The minimum and maximum values of PID controller parameters are chosen as -2.0 and 2.0 respectively. The range for filter coefficient N is selected as 1 and 300 [19]. The ACE minimization for optimal values of PIDF controller coefficients has been solved using the BBBC search algorithm. The performance of the proposed controller has also been compared with other PI controller.

3.2. Over view of the Big Bang Big Crunch (BBBC) algorithms

The Big Bang and Big Crunch theory are introduced by Erol and Eksin [13], which is based upon the analogy of universe evolution where two phase of evolution is represented by expansion (Big Bang) & contraction (Big crunch). This algorithm has a low computational time and high convergence speed. In fact, the Big Bang phase dissipates energy and produces disorder and randomness. In the Big Crunch phase, randomly distributed particles (which form the solution when represented in a problem) are arranged into an order by way of a convergence operator "centre of mass". The Big Bang–Big Crunch phases are followed alternatively until randomness within the search space during the Big Bang becomes smaller, smaller, and finally leading to a solution. The following steps have discussed the algorithm for the BBBC. (i) Create random population of solution, (ii) Evaluate Solutions, (iii) The fittest individual can be selected as the centre of mass, (iv) Calculate new candidates around the centre of mass by adding or subtracting a normal random number whose value decreases as the iterations elapse, (v) The algorithm continues until predefined stopping criteria has been met.

3.3. Design of PIDF controller using BBBC algorithms

The algorithm is inspired by the big bang theory. The BBBC algorithm produces random points in the search space and shrinks those points to a single solution point [13, 14, 22]. The proposed BBBC algorithm for solving AGC application. Consider PIDF controller for each are

Step1: Consider PIDF controller for each area and generated population for each parameter

$$x_{ij}^k = {x_i}_{min}^k + rand * \left({x_i}_{max}^k - {x_i}_{min}^k\right) \quad (12)$$

where $x = [K_P, K_I, K_{D,} N]$, represents the PIDF controller parameters. k = [1, 2] represents the total number of areas, i = [1, 2, 3 and 4], shows the number of each controller parameter and j= [1, 2, 3...30], determines the population size. x_i^{min} and x_i^{max} are the upper and lower limit of i^{th} parameters. This is called the big bang phase.

Step 2: Determine the objective function value as given in Eq. (9) for each population.

Step 3: Computation of the centre of mass on the basis of the current position of each parameter in the population and the associated fitness function value as given by Eq. (13), where X_{comp}, position vector of centre of mass

$$X_{com} = \frac{\sum_{j=1}^{p} \frac{x_{ij}^k}{F_j}}{\sum_{j=1}^{p} \frac{1}{F_j}} \tag{13}$$

Step 4: This step considers the generation of a new population for each controller parameter in the vicinity of the centre of mass using Eq.(14).

$$x_{ij}{}_{new}^{k} = \beta X_{com} + (1-\beta)x_{best} + \frac{rand*\alpha(x_i{}_{max}^{k} - x_i{}_{min}^{k})}{iteration} \tag{14}$$

where $\alpha$is the parameter limiting the size of the search space and $\beta$is the parameter controlling the influence of global best solution x_{best} on the location of the new candidate solution.

Step 5: Calculation of the fitness function of these newly generated parameters and compares with earlier fitness function value and compute minimum fitness function and corresponding parameters selected as the next parameters.

$$x_{ij}{}_{next}^{k} = min\left\{F\left(x_{ij}^{k}(\text{earlier})\right), F\left(x_{ij}^{k}(new)\right)\right\} \tag{15}$$

Step 6: Calculate the difference between the new and earlier fitness value for all generations

If $e_{ij}^{k} = \left(x_{ij}^{k}(new) - x_{ij}^{k}(\text{earlier})\right)$ and $e_{ij}^{k} < 10^{-4}$ then stop, it gives optimum fitness value which results the optimum parameters of PIDF controller for AGC loop otherwise go to step 2.

4. Function HES and IPFC unit in AGC loop

4.1. Schematic diagram of Hydrogen Energy Storage (HES)

The hydrogen energy storage is a process of splitting the water into hydrogen and oxygen by giving the direct current to the electrodes in an electrolysis cells; hydrogen is then compressed into a tank, so that energy can be stored in the form of hydrogen gas, then the hydrogen energy is converted back to electricity by fuel cells and few other types of equipment. Fuel cells are devices normally used to convert hydrogen energy back into electricity for easy operation and higher efficiency compared with other devices used to convert the hydrogen to electricity. The important elements of a HES unit comprise an Electrolyser unit, which converts electrical energy input into hydrogen by decomposing water molecules, the hydrogen storage system itself and a hydrogen energy conversion system, which converts the stored chemical energy in the hydrogen back to electrical energy as shown in Fig. 4. The transfer function of the Aqua Electrolyser can be expressed as first order lag:

$$G_{AE}(s) = \frac{K_{AE}}{1+sT_{AE}} \tag{16}$$

The transfer function of Fuel Cell (FC) can be given by a simple linear equation as

$$G_{FC}(s) = \frac{K_{FC}}{1+sT_{FC}} \tag{17}$$

The overall transfer function of hydrogen Energy storage unit has can be

$$G_{HES}(s) = \frac{K_{HES}}{1+sT_{HES}} = \frac{K_{AE}}{1+sT_{AE}} * \frac{K_{FC}}{1+sT_{FC}} \tag{18}$$

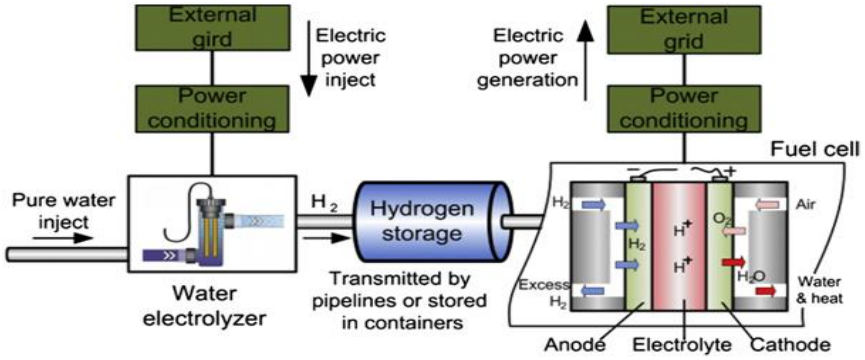

Fig. 4. Schematic diagram of the hydrogen Energy storage unit.

4.2. Schematic diagram of IPFC unit

The Interline Power Flow Controller (IPFC) employs a number of voltage source converters each providing series compensation for a different line. Figure 5 shows the schematic diagram of IPFC. The simplest IPFC consist of two back-to-back dc-to-ac converters, which are connected in series with two transmission lines through series coupling transformers and the dc terminals of the converters are connected together via a common dc link. With this scheme, in addition to providing series reactive compensation, any converter can be controlled to supply real power to the common dc link from its own transmission line [22, 23].

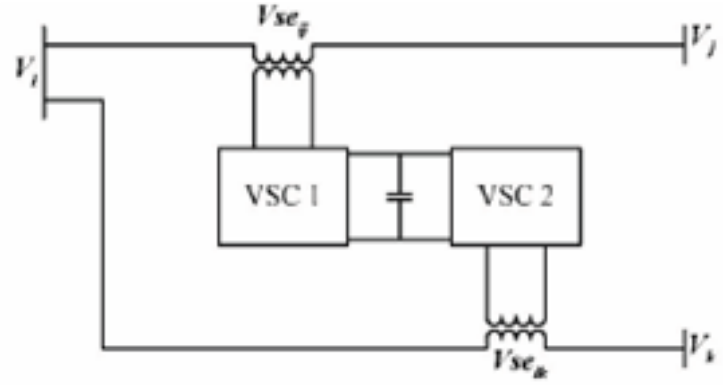

Fig. 5. Schematic diagram IPFC unit.

5. Control Design for HES and IPFC unit in AGC Loop

The Linearized reduction model test system with HES and IPFC units for the control design is shown in Fig. 6, where the forceful of governor system is eradicated by setting the mechanical inputs as constant since the response of governor is much slower than that of HES or IPFC units. From the physical viewpoint, it is noted that the IPFC located between two areas is successful to stabilize the inter-area oscillation mode only, and then the HES, which is capable of supplying the energy into the power system, should be suitable for the control of the inertia mode.

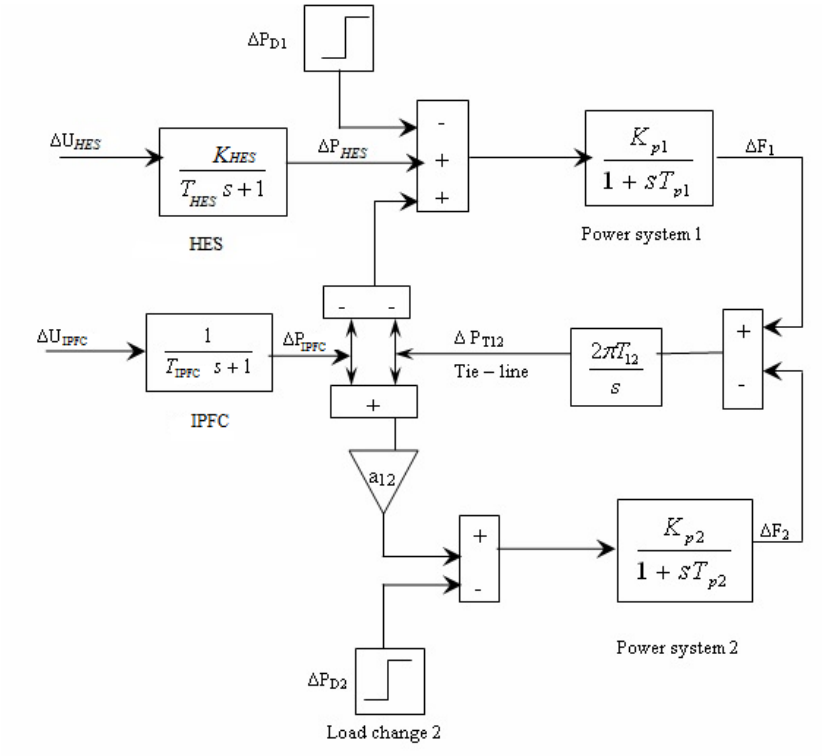

Fig. 6. Linearized reduction model for the test system with HES and IPFC units.

The HES is modelled as an active power source to area 1 with the gain constant K_{HES} and time constant T_{HES}. The IPFC is modelled as a tie-line power flow controller with a time constant $T_{IPFC.}$ From Fig. 6, the state equations are derived as follows.

$$\begin{bmatrix} \Delta\dot{F}_1 \\ \Delta\dot{P}_{T12} \\ \Delta\dot{F}_2 \end{bmatrix} = \begin{bmatrix} -1/T_{p1} & -k_{p1}/T_{p1} & 0 \\ 2\pi T_{12} & 0 & -2\pi T_{12} \\ 0 & a_{12}\,k_{p2}/T_{p2} & -1/T_{p2} \end{bmatrix} \begin{bmatrix} \Delta F_1 \\ \Delta P_{T12} \\ \Delta F_2 \end{bmatrix} + \begin{bmatrix} k_{p1}/T_{p1} & -k_{p1}/T_{p1} \\ 0 & 0 \\ 0 & a_{12}\,k_{p2}/T_{p2} \end{bmatrix} \begin{bmatrix} \Delta P_{HES} \\ \Delta P_{IPFC} \end{bmatrix} \quad (19)$$

5.1. Control design of HES unit:

The design process starts with the reduction of two-area system into one area, which represents the Inertia centre mode of the overall system. The controller of HES is designed in the equivalent one area system to reduce the frequency deviation of inertia centre. The equivalent system is derived by assuming the synchronizing coefficient T_{12} to be large. From the state equation of $\Delta\dot{P}_{T12}$ in Eq. (19)

$$\frac{\Delta\dot{P}_{T12}}{2\pi T_{12}} = \Delta F_1 - \Delta F_2 \tag{20}$$

Let us assume Synchronous coefficient (T_{12}) is infinity, then Eq. (20) becomes $\Delta F_1 = \Delta F_2$. Expanding in Eq. (19), $\Delta\dot{F}_1$ and $\Delta\dot{F}_2$ multiplying by T_{p1}/k_{p1} and $T_{p2}/a_{12}k_{p2}$ respectively

$$(T_{p1}/k_{p1})\,\Delta\dot{F}_1 = -(1/k_{p1})\Delta F_1 - \Delta P_{T12} + \Delta P_{HES} - \Delta P_{IPFC} \tag{21}$$

$$(T_{p2}/a_{12}k_{p2})\,\Delta\dot{F}_2 = -(1/a_{12}k_{p2})\Delta F_2 + \Delta P_{T12} + \Delta P_{IPFC} \tag{22}$$

Sub $\Delta F_1 = \Delta F_2 = \Delta F$ and summing Eq. (21) and (22) we get

$$\Delta\dot{F} = \left(-1/k_{p1} - (1/a_{12}k_{p2})\right)/\left((T_{p1}/k_{p1}) + (T_{p2}/a_{12}k_{p2})\right) + \left(1/\left((T_{p1}/k_{p1}) + (T_{p2}/a_{12}k_{p2})\right)\right)\Delta P_{HES} + C\Delta P_D \tag{23}$$

The load change in this system ΔP_D is additionally considered, where C is constant, here the control $\Delta P_{HES} = -K_{HES}\,\Delta F$ is applied then.

$$\Delta F = \frac{C}{s + A + K_{HES}B}\Delta P_D \tag{24}$$

where $A = \left(-1/k_{p1} - (1/a_{12}k_{p2})\right)/\left((T_{p1}/k_{p1}) + (T_{p2}/a_{12}k_{p2})\right)$

$B = 1/\left((T_{p1}/k_{p1}) + (T_{p2}/a_{12}k_{p2})\right)$;

C is the proportionality between change in frequency and change in load demand.

In Eq. (24) the final values with K_{HES} =0 and $K_{HES} \neq 0$ are C/A and $C / (A+K_{HES} B)$ respectively therefore the percent reduction is represented by

$$(C/A + K_{HES}\,B)/(C/A) = R/100 \tag{25}$$

The control gain of HES unit is expressed as

$$K_{HES} = (A/BR) * (100 - R) \tag{26}$$

5.2. Control design of Interline power flow controller

The controller for the IPFC is intended to improve the damping of the inter-area mode. In order to extract the inter-area mode from the system Eq. (19), the concept of overlapping decompositions is applied. Then, one subsystem, which preserves the inter-area mode, is represented by

$$\begin{bmatrix}\Delta\dot{F}_1 \\ \Delta P_{T12}\end{bmatrix} = \begin{bmatrix}-1/T_{p1} & -k_{p1}/T_{p1} \\ 2\pi T_{12} & 0\end{bmatrix}\begin{bmatrix}\Delta F_1 \\ \Delta P_{T12}\end{bmatrix} + \begin{bmatrix}-k_{p1}/T_{p1} \\ 0\end{bmatrix}[\Delta P_{IPFC}] \tag{27}$$

The controlling purpose of the IPFC is to damp the peak value of frequency deviation in area 1 after a sudden change in the load demand. Since the system Eq. (27) is the second order oscillation system, the percentage overshoot *Mp*

(new) can be specified for the control design. *Mp (new)* is given as a function of the damping ratio by

$$M_{Pnew} = e^{\left(-\pi\delta/\sqrt{1-\delta^2}\right)} \tag{28}$$

The real and imaginary parts of Eigen value after the control are expressed as $\alpha_s = \delta\omega_n$ and $\beta_s = \omega_{n\sqrt{1-\delta^2}}$, where w_n is the undamped natural frequency, by specifying *Mp* and assuming $\beta_s = \beta$, the desired pair of an Eigen value is fixed. As a result, the Eigen value assignment method derives to feedback scheme as

$$\Delta P_{IPFC} = -k_1\Delta F_1 - k_2\Delta P_{T12} \tag{29}$$

6. Evaluation Power System Ancillary Service Requirement (ASR) Indices

Power system restoration is well-known procedure to reduce the impact of a disturbance generally occurs in power systems. The high-level approach of the system restoration plan is to restore the integrity of the interconnection as quickly as possible. The system restoration strategies are originating in the system's characteristics. After analysing the system conditions and characteristics of outages, the system restoration planners or dispatchers will select the power system Ancillary Service Requirement (ASR) indices, which are obtained from system dynamic performances, and the remedial measures to be taken can be adjudged. The various power system Ancillary System Restoration indices (ASR_1, ASR_2, ASR_3, and ASR_4) are calculated as follows

Step 1: The ASR_1 is obtained from difference between the peak value of the control input deviation of area 1 $\Delta P_{C1}(\tau_P)$ and steady state value of control input deviation $\Delta P_{C1}(\tau_s)$

$$ASR_1 = \Delta P_{c1}(\tau_p) - \Delta P_{c1}(\tau_s) \tag{30}$$

Step 2: The ASR_2 is obtained from the difference between peak value of the control input deviation of area 2 $\Delta P_{C2}(\tau_P)$ and steady state value of control input deviation $\Delta P_{C2}(\tau_s)$

$$ASR_2 = \Delta P_{c2}(\tau_p) - \Delta P_{c2}(\tau_s) \tag{31}$$

Step 3: The ASR_3 is obtained from difference between the maximum and steady state value of the mechanical power generation deviation of $Genco_1$

$$ASR_3 = \Delta P_{M1}(\tau_p) - \Delta P_{M1}(\tau_s) \tag{32}$$

Step 4: The ASR_4 is obtained from difference between the maximum and steady state value of the mechanical power generation deviation of $Genco_2$

$$ASR_4 = \Delta P_{M2}(\tau_p) - \Delta P_{M2}(\tau_s) \tag{33}$$

Step 5: The ASR_5 is obtained from difference between the maximum and steady state value of the mechanical power generation deviation of $Genco_3$

$$ASR_5 = \Delta P_{M3}(\tau_p) - \Delta P_{M3}(\tau_s) \tag{34}$$

Step 6: The ASR_6 is obtained from difference between the maximum and steady state value of the mechanical power generation deviation of $Genco_4$

$$ASR_6 = \Delta P_{M4}(\tau_p) - \Delta P_{M4}(\tau_s) \tag{35}$$

7. Simulation Results and Observations

In this study two-area, thermal-thermal power system is pain staked for the investigation with different generation schedules. Each area consists of two Gencos units and each Gencos unit have identical steam turbines with 500MW capacities. The model of the system under study has been developed in MATLAB/SIMULINK environment. The nominal parameters are given in *Appendix A*. In this study, Big Bang Big Crunch (BBBC) algorithm is used for optimal tuning PIDF controller for AGC loop of a two-area thermal deregulated power system with reheat bicycle mix condensation turbine. The optimal solution of control inputs is taken for optimization problem and the objective function in Eq. (9) is derived using the frequency deviations of control areas and tie-line power changes. The active power model of IPFC unit is fitted in the tie-line near area1 and HES unit is installed in area1 to examine its effect on the power system performance.

The gain values of HES unit is K_{HES}=0.902 using Eq. (26) for the given value of speed regulation coefficient (R). The purpose of incorporating IPFC unit is to damp out the peak value of frequency deviations in both areas and tie-line power deviations. Since the system Eq. (27) is second order oscillations system, the feedback gains k_1 and k_2 are found using Eq. (29) for a specified peak overshoot *Mp (new).* The feedback gain values IPFC is k_1= -0.645 and k_2= -1.08 for *Mp (new)*= 2%. The optimum PIDF controller gain values of test system without and with HES and IPFC unit for various case studies are listed in the Tables 1 and 2.

These PIDF controllers are implemented in a proposed test system for different types of transactions with different generation schedules and compared with PI controller. The dynamic model steam turbine parameters have been used AGC loop under varying generation schedule condition. The corresponding ASR indices are calculated using Eqs. (30)-(35) from dynamic responses of control input deviations, and mechanical power generation deviations of each area for different types of possible transactions of the proposed test system.

Scenario 1: Poolco based transaction

In this scenario, Gencos participate only in the load following control of their areas. It is assumed that a large step load 0.15*p.u*MW is demanded by each Disco in area 1. Assume that a case of Poolco based contracts between Dicos and available Gencos is simulated based on the following Disco Participation Matrix (DPM) referring to Eq. (1) is considered as

$$DPM = \begin{bmatrix} 0.5 & 0.5 & 0.0 & 0.0 \\ 0.5 & 0.5 & 0.0 & 0.0 \\ 0.0 & 0.0 & 0.0 & 0.0 \\ 0.0 & 0.0 & 0.0 & 0.0 \end{bmatrix} \tag{36}$$

$Disco_1$ and $Disco_2$ demand identically from their local Gencos, viz., $Genco_1$ and $Genco_2$. Therefore, $cpf_{11} = cpf_{12} = 0.5$ and $cpf_{21} = cpf_{22} = 0.5$. It may happen that a Disco violates a contract by demanding more power than that specified in the contract and this excess power is not contracted to any of the Gencos. This uncontracted power must be supplied by the Gencos in the same area to the Disco. It is represented as a local load of the area but not as the contract demand. Consider scenario-1 again with a modification that Disco demands as given in Tables 1 and 2. From the simulation results, ASR Indices are evaluated using Eqs. (30)-(35) from dynamic responses of the control input deviations and mechanical power generation deviations of each area

for the proposed test system without and with HES and IPFC unit is shown in Tables 3 to 5 (Cases 1 to 4). From Fig. 7 and Tables 3 to 5, the overall system performance in terms of settling times and peak overshoots are also greatly improved with proposed BBBC algorithm optimized PIDF controller compared to PI controller. Moreover, the dynamic performance and ASR indices are improved with the coordinated application of HES and IPFC units.

Scenario 2: Bilateral transaction

Here all the Discos have a contract with the Gencos and the following Disco Participation Matrix (DPM) referring to Eq. (1) is considered as

$$DPM = \begin{bmatrix} 0.1 & 0.0 & 0.2 & 0.5 \\ 0.4 & 0.4 & 0.2 & 0.0 \\ 0.3 & 0.0 & 0.3 & 0.3 \\ 0.2 & 0.6 & 0.3 & 0.2 \end{bmatrix} \tag{37}$$

In this case, the $Disco_1$, $Disco_2$, $Disco_3$ and $Disco_4$, demands of 0.1 pu.MW for each from Gencos as defined by cpfin the DPM matrix and each Gencos participates in AGC as defined by the following ACE participation factor $apf_{11} = apf_{12} = 0.5$ and $apf_{21} = apf_{22} = 0.5$. The corresponding ASR indices are calculated using Eqs. (30)-(35) from dynamic responses of control input deviations and mechanical power generation deviations of each area of the proposed test system without and with HES and IPFC units are shown in Tables 3 to 5 (Cases 5 to 8). Apart from the normal operating condition of the test systems, few other case studies like outage generating unit in any area and uncontracted power demand in any area during the outage are also considered. In this study $Genco_2$ in area 1 is an outage and uncontracted power demand in any area and Disco Participation Matrix Eq. (37) is considered. From simulation results, the ASR indices are evaluated in the proposed test system and tabulated in Tables 3 to 5 (Cases 9 to 12). From these ASR Indices, the restorative measures like the magnitude of control input and, mechanical power generation deviations of each area required can be adjudged. From the simulated results is shown in Fig. 8. It is observed that the restoration process with the HES and IPFC units ensures not only reliable operation but provides a good margin of stability compared with the test system without HES and IPFC units. The main focus in this paper ASR index is useful for system planners for restoration planning in advance.

(i) If $0.3 \leq ASR_1, ASR_2 \leq 0.5$, then the system subject to a large steady error for step load changes. The integral control action is required based on the performance criteria. The integral controller gain of each control area has to be increased causing the speed changer valve to open up widely. Thus, the speed- changer position attains a constant value only when the frequency error is reduced to zero.

(ii) If $ASR_1, ASR_2 \geq 0.5$, then the system required more amount of distributed generation requirement is needed and the FACTS devices are needed to improvement tie-line power oscillations.

(iii) If $0.02 \leq ASR_3, ASR_4, ASR_5, ASR_6 \leq 0.05$, then the system required the stabilization of frequency oscillations in an interconnected power system. The conventional load-frequency controller may no longer be able to attenuate the large frequency oscillation due to the slow response of the governor for unpredictable load variations.Thus continuing change in power system configurations and their operating conditions might lead to undesired operation of relays. So that in a deregulated system, regulation and load following are the

two frequency-related ancillary services required for balancing the varying load with matching generation. In cases where a dramatic decline in frequency occurs during the restoration process, it is necessary to reduce the amount of load that is connected, which can be accomplished by the application of under load shedding scheme.

(iv) If $ASR_3, ASR_4, ASR_5, ASR_6 \geq 0.05$, then the system is vulnerable and the system becomes unstable and may result to blackout. To restore the system as quickly as possible, especially for a bulk system, partitioning system into islands is necessary. Islands are resynchronized after the restoration of each island. Major actions involved in this restoration process are start-up of black start units, cranking of non-black start units, restoration of islands, and synchronization of islands.

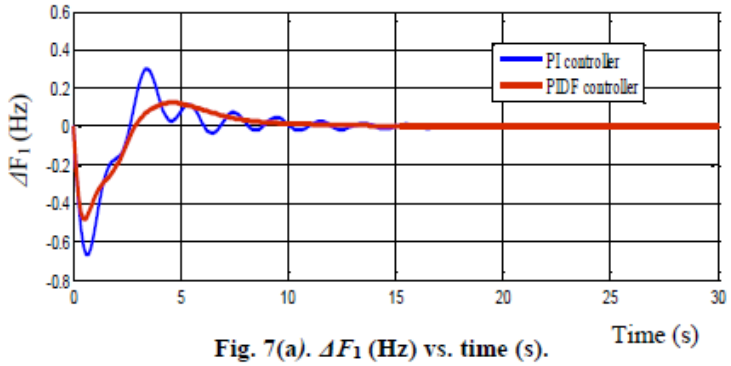

Fig. 7(a). ΔF_1 (Hz) vs. time (s).

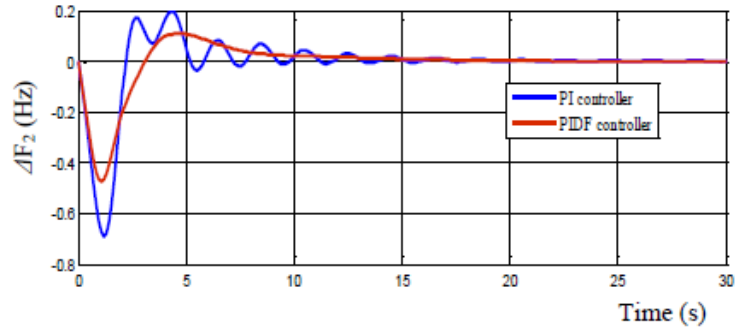

Fig. 7(b). ΔF_2 (Hz) vs. time (s).

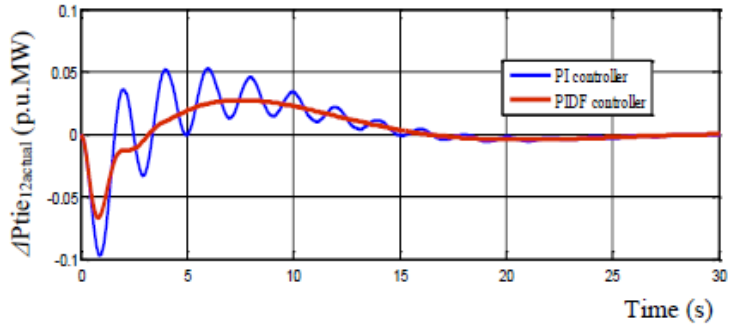

Fig. 7(c). $\Delta Ptie_{12,\,actual}$ (p.u.MW) vs. time (s).

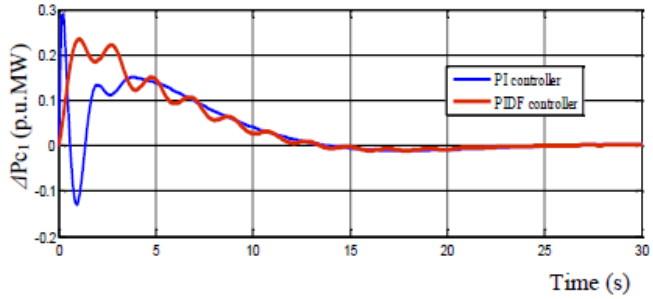

Fig. 7(d). ΔP_{C1} (p.u.MW) vs. time (s).

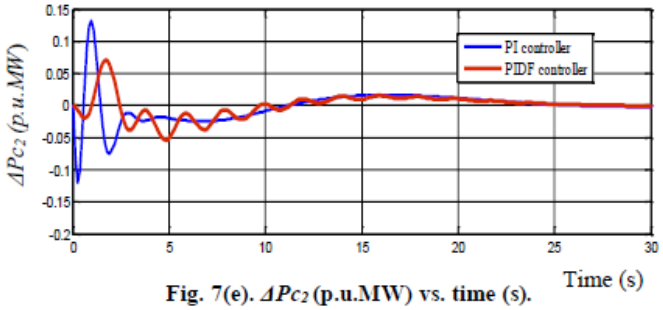

Fig. 7(e). ΔP_{C2} (p.u.MW) vs. time (s).

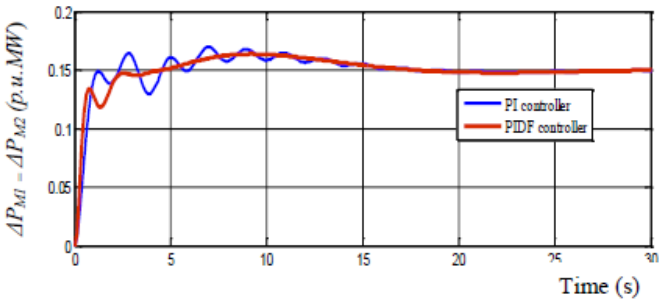

Fig. 7(f). $\Delta P_{M1} = \Delta P_{M2}$ (p.u.MW) vs. time (s).

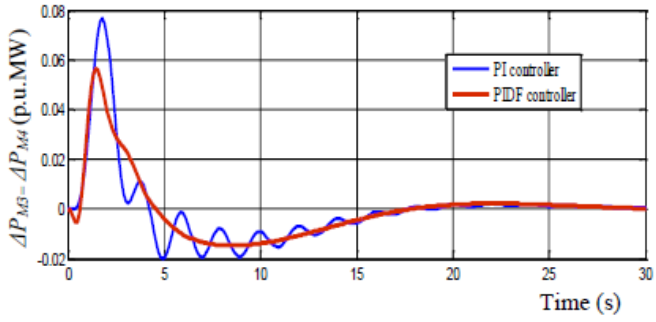

Fig. 7(g). $\Delta P_{M3} = \Delta P_{M4}$ (p.u.MW) vs. time (s).

Fig. 7. Dynamic responses of the frequency deviations, tie-line power deviations, Control input deviations and mechanical power generation deviations for a two-area thermal-thermal system using PI and PIDF controllers (case-1).

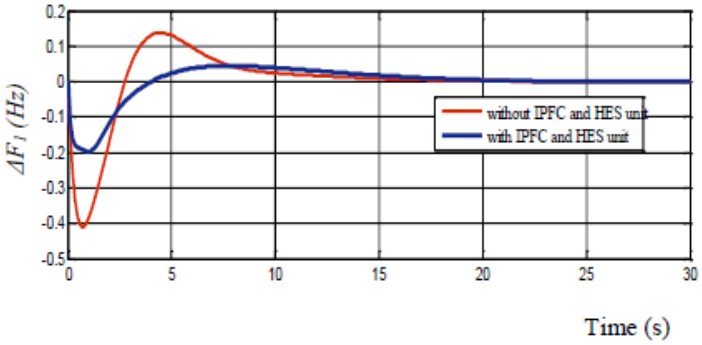

Fig. 8(a). ΔF_1 (Hz) vs. time (s).

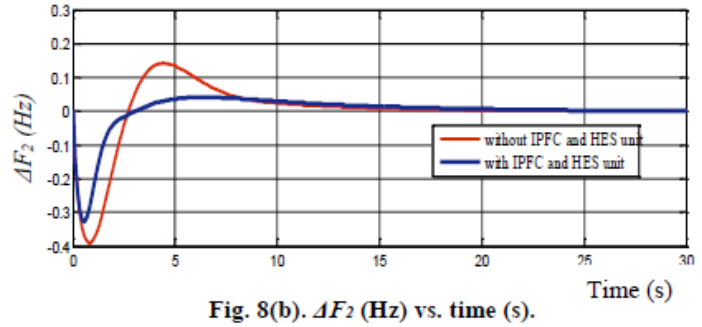

Fig. 8(b). ΔF_2 (Hz) vs. time (s).

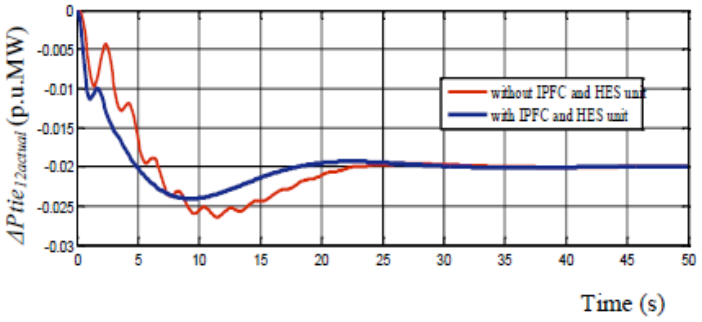

Fig. 8(c). $\Delta Ptie_{12,\ actual}$ (p.u.MW) vs. time (s).

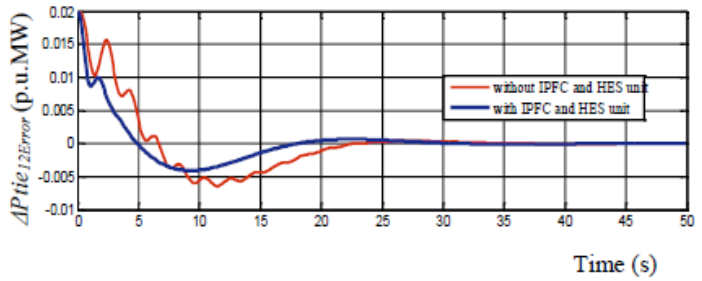

Fig. 8(d). $\Delta Ptie_{12,\ Error}$ (p.u.MW) vs. time (s).

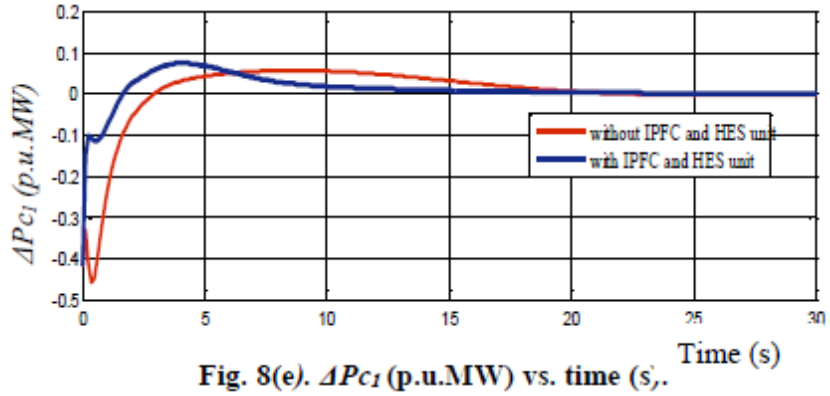

Fig. 8(e). ΔP_{C1} (p.u.MW) vs. time (s).

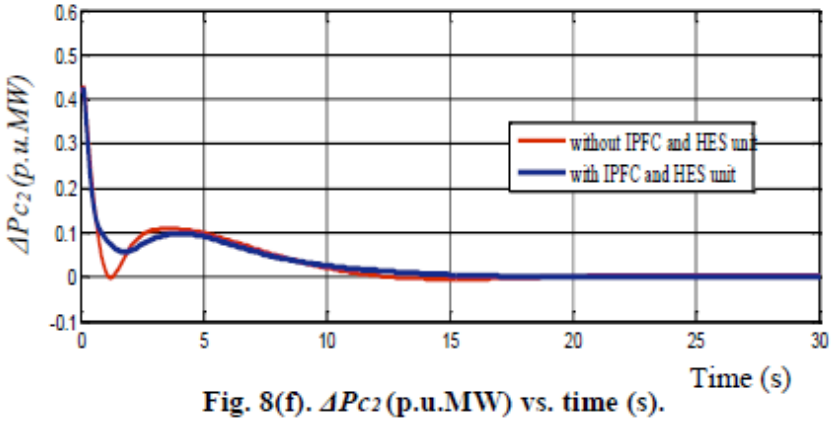

Fig. 8(f). ΔP_{C2} (p.u.MW) vs. time (s).

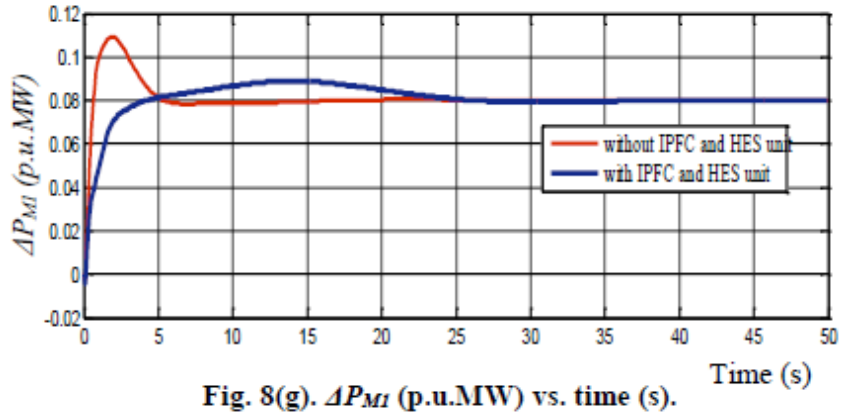

Fig. 8(g). ΔP_{M1} (p.u.MW) vs. time (s).

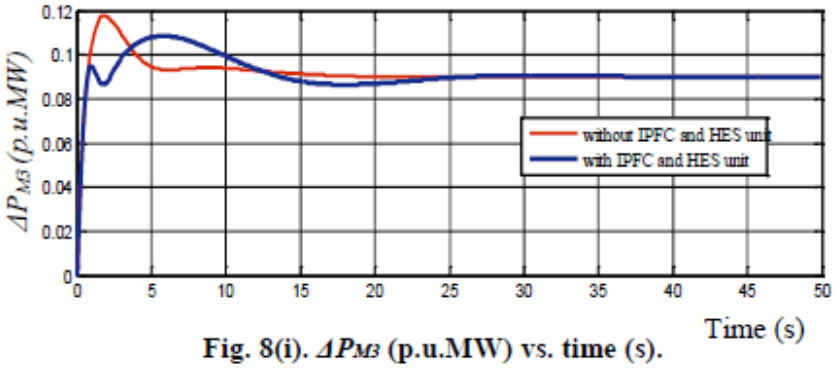

Fig. 8(i). ΔP_{M3} (p.u.MW) vs. time (s).

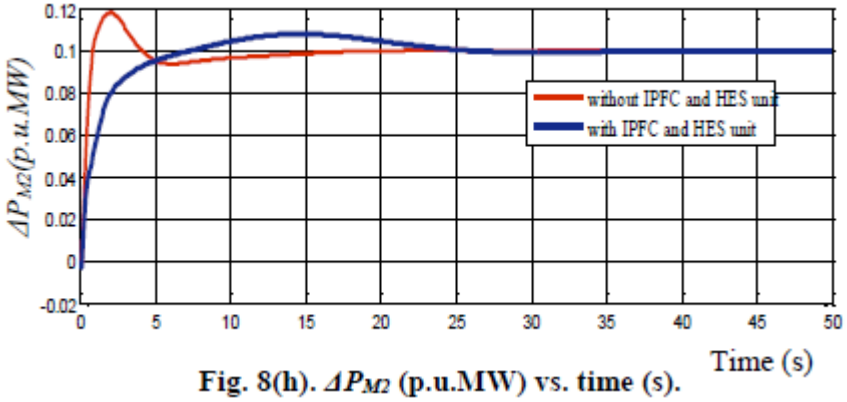

Fig. 8(h). ΔP_{M2} (p.u.MW) vs. time (s).

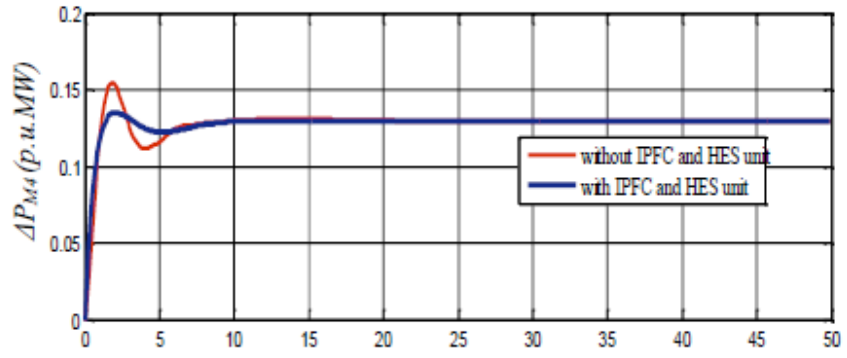

Fig. 8(j). ΔP_{M4} (p.u.MW) vs. time (s).

Fig. 8. Dynamic responses of the frequency deviations, tie-line power deviations, control input deviations and mechanical power generation deviations for a two-area thermal-thermal system without and with IPFC and HES units (Case-5).

Table 1. Optimal PIDF controller gain values using BBBC algorithm for two-area thermal-thermal power system with corresponding change in load demand.

Two-area thermal-thermal system	PIDF controller gain of area 1				PIDF controller gain of area 2				Load demand in pu.MW			
	K_P	K_I	K_D	N	K_P	K_I	K_D	N	$Disco_1$	$Disco_2$	$Disco_3$	$Disco_4$
Case 1	0.324	0.497	0.823	25.36	0.315	0.463	0.514	23.36	0.15	0.15	0.0	0.0
Case 2	0.367	0.523	0.945	30.45	0.324	0.475	0.527	21.57	0.15	0.15	0.0	0.0
Case 3	0.334	0.481	0.875	26.47	0.341	0.486	0.601	24.49	0.15	0.15	0.0	0.0
Case 4	0.381	0.647	0.972	32.78	0.457	0.642	0.513	35.69	0.15	0.15	0.0	0.0
Case 5	0.311	0.408	0.623	22.54	0.302	0.437	0.498	22.78	0.10	0.10	0.10	0.10
Case 6	0.323	0.426	0.708	28.64	0.311	0.441	0.507	23.97	0.10	0.10	0.10	0.10
Case 7	0.318	0.404	0.629	23.85	0.387	0.524	0.647	25.61	0.10	0.10	0.10	0.10
Case 8	0.354	0.478	0.845	28.47	0.412	0.645	0.784	28.66	0.10	0.10	0.10	0.10
Case 9	0.364	0.523	0.975	33.78	0.547	0.754	0.978	35.78	0.15	0.05	0.15	0.05
Case 10	0.428	0.642	0.998	40.12	0.552	0.767	0.988	36.48	0.15	0.05	0.15	0.05
Case 11	0.437	0.652	0.912	40.78	0.612	0.783	0.942	38.45	0.15	0.05	0.15	0.05
Case 12	0.442	0.752	0.933	33.78	0.645	0.842	0.991	40.23	0.15	0.05	0.15	0.05

Table 2. Optimal PIDF controller gain values using BBBC algorithm for two-area thermal-thermal power system with IPFC and HES unit for corresponding change in load demand.

Two-area thermal-thermal system	PIDF controller gain of area 1				PIDF controller gain of area 2				Load demand in pu.MW			
	K_P	K_I	K_D	N	K_P	K_I	K_D	N	$Disco_1$	$Disco_2$	$Disco_3$	$Disco_4$
Case 1	0.313	0.484	0.812	26.13	0.306	0.443	0.428	26.18	0.15	0.15	0.0	0.0
Case 2	0.354	0.518	0.923	32.22	0.313	0.453	0.454	24.33	0.15	0.15	0.0	0.0
Case 3	0.322	0.469	0.868	28.37	0.337	0.469	0.556	27.23	0.15	0.15	0.0	0.0
Case 4	0.375	0.637	0.963	30.54	0.443	0.626	0.426	38.54	0.15	0.15	0.0	0.0
Case 5	0.303	0.401	0.614	26.62	0.297	0.426	0.378	26.62	0.10	0.10	0.10	0.10
Case 6	0.315	0.414	0.695	25.73	0.303	0.423	0.405	26.58	0.10	0.10	0.10	0.10
Case 7	0.305	0.398	0.612	22.91	0.364	0.509	0.523	26.73	0.10	0.10	0.10	0.10
Case 8	0.332	0.454	0.823	26.57	0.402	0.618	0.676	29.54	0.10	0.10	0.10	0.10
Case 9	0.344	0.506	0.963	36.74	0.538	0.732	0.863	38.12	0.15	0.05	0.15	0.05
Case 10	0.403	0.637	0.994	44.28	0.545	0.743	0.872	39.08	0.15	0.05	0.15	0.05
Case 11	0.422	0.649	0.894	42.12	0.608	0.764	0.833	40.64	0.15	0.05	0.15	0.05
Case 12	0.434	0.749	0.911	36.45	0.632	0.839	0.876	44.06	0.15	0.05	0.15	0.05

Table 3. ASR indices for two-area thermal-thermal power system without and with HES and IPFC units considering 100 % Generation schedules.

Load demand change	ASR indices for two area thermal-thermal system without HES and IPFC unit						ASR indices for two area thermal-thermal system with HES and IPFC unit					
	ASR_1	ASR_2	ASR_3	ASR_4	ASR_5	ASR_6	ASR_1	ASR_2	ASR_3	ASR_4	ASR_5	ASR_6
Case 1	0.298	0.144	0.015	0.014	0.076	0.075	0.239	0.075	0.013	0.012	0.026	0.025
Case 2	0.302	0.171	0.017	0.015	0.081	0.080	0.254	0.101	0.014	0.013	0.027	0.026
Case 3	0.317	0.184	0.016	0.016	0.085	0.085	0.262	0.113	0.015	0.015	0.029	0.028
Case 4	0.324	0.198	0.022	0.021	0.094	0.093	0.288	0.201	0.019	0.017	0.031	0.032
Case 5	0.461	0.435	0.031	0.019	0.029	0.013	0.352	0.412	0.011	0.014	0.022	0.011
Case 6	0.472	0.442	0.032	0.021	0.032	0.014	0.356	0.416	0.013	0.015	0.023	0.014
Case 7	0.474	0.456	0.038	0.023	0.036	0.016	0.361	0.422	0.015	0.016	0.025	0.016
Case 8	0.489	0.462	0.041	0.029	0.039	0.021	0.368	0.426	0.016	0.017	0.027	0.017
Case 9	0.491	0.473	0.043	0.031	0.041	0.025	0.372	0.428	0.018	0.021	0.028	0.019
Case 10	0.496	0.476	0.045	0.036	0.042	0.027	0.375	0.429	0.021	0.022	0.031	0.022
Case 11	0.499	0.496	0.046	0.039	0.045	0.032	0.378	0.431	0.023	0.024	0.033	0.025
Case 12	0.512	0.498	0.051	0.042	0.053	0.036	0.417	0.434	0.028	0.026	0.035	0.026

Table 4. ASR indices for two-area thermal-thermal power system without and with HES and IPFC units considering 80 % Generation schedules.

Load demand change	ASR indices for two area thermal-thermal system without HES and IPFC unit						ASR indices for two area thermal-thermal system with HES and IPFC unit					
	ASR_1	ASR_2	ASR_3	ASR_4	ASR_5	ASR_6	ASR_1	ASR_2	ASR_3	ASR_4	ASR_5	ASR_6
Case 1	0.382	0.201	0.032	0.031	0.081	0.079	0.355	0.122	0.024	0.023	0.042	0.041
Case 2	0.388	0.216	0.034	0.033	0.084	0.083	0.362	0.131	0.026	0.025	0.044	0.043
Case 3	0.392	0.227	0.036	0.035	0.084	0.083	0.369	0.133	0.027	0.026	0.045	0.044
Case 4	0.398	0.231	0.038	0.036	0.088	0.087	0.371	0.142	0.028	0.028	0.047	0.046
Case 5	0.472	0.442	0.036	0.021	0.032	0.016	0.361	0.424	0.021	0.024	0.028	0.015
Case 6	0.475	0.462	0.038	0.022	0.033	0.018	0.368	0.429	0.023	0.026	0.029	0.016
Case 7	0.478	0.468	0.041	0.024	0.037	0.019	0.371	0.431	0.025	0.027	0.031	0.017
Case 8	0.494	0.471	0.043	0.025	0.039	0.021	0.372	0.432	0.027	0.029	0.032	0.018
Case 9	0.498	0.475	0.048	0.027	0.041	0.023	0.375	0.438	0.028	0.031	0.033	0.021
Case 10	0.499	0.478	0.049	0.032	0.046	0.029	0.385	0.445	0.031	0.032	0.038	0.025
Case 11	0.500	0.481	0.055	0.039	0.049	0.034	0.394	0.446	0.032	0.033	0.039	0.028
Case 12	0.523	0.514	0.059	0.048	0.055	0.046	0.421	0.448	0.033	0.036	0.045	0.029

Table 5. ASR indices for two-area thermal-thermal power system without and with HES and IPFC units considering 50 % Generation schedules.

Load demand change	ASR indices for two area thermal-thermal system without HES and IPFC unit						ASR indices for two area thermal-thermal system with HES and IPFC unit					
	ASR_1	ASR_2	ASR_3	ASR_4	ASR_5	ASR_6	ASR_1	ASR_2	ASR_3	ASR_4	ASR_5	ASR_6
Case 1	0.423	0.292	0.041	0.040	0.092	0.091	0.382	0.157	0.031	0.030	0.053	0.051
Case 2	0.426	0.294	0.043	0.042	0.093	0.092	0.391	0.159	0.035	0.034	0.055	0.054
Case 3	0.428	0.296	0.048	0.047	0.095	0.094	0.394	0.162	0.037	0.036	0.057	0.056
Case 4	0.451	0.304	0.049	0.048	0.096	0.096	0.395	0.166	0.038	0.037	0.058	0.057
Case 5	0.481	0.451	0.041	0.026	0.035	0.017	0.373	0.444	0.025	0.028	0.031	0.019
Case 6	0.483	0.463	0.043	0.028	0.037	0.018	0.378	0.454	0.028	0.031	0.035	0.021
Case 7	0.485	0.468	0.045	0.029	0.038	0.021	0.381	0.463	0.029	0.032	0.036	0.023
Case 8	0.501	0.475	0.046	0.031	0.041	0.022	0.385	0.475	0.031	0.035	0.038	0.028
Case 9	0.502	0.489	0.047	0.035	0.042	0.027	0.388	0.478	0.032	0.036	0.039	0.029
Case 10	0.507	0.501	0.051	0.037	0.044	0.029	0.391	0.482	0.034	0.038	0.041	0.031
Case 11	0.511	0508	0.052	0.041	0.046	0.031	0.398	0.486	0.037	0.039	0.043	0.033
Case 12	0.537	0.523	0.061	0.049	0.055	0.046	0.429	0.491	0.038	0.041	0.048	0.039

8. Conclusion

The PIDF controllers are formulated to use BBBC algorithm and realized in two area interconnected power system without and with HES and IPFC units for different types of transactions under different generation scheduled. The various simulated results show that the BBBC algorithm based PIDF controller's performance is swift, more accurate and better than the simulated results with PI controllers. HES unit is included in area 1 along with IPFC unit in the tie-line in order to improve the system performance. It is observed that in all the cases (poolco based, bilateral based and contract violation based) the deviation of frequency becomes zero in the steady state with less setting time because of the coordinated application of HES and IPFC units which assures the prime requirement of AGC. The study also reveals that the BBBC algorithm is more accurate, reliable and efficient in finding the global optimal solution than other optimization algorithms. The proposed PIDF controller with AGC system has HES and IPFC units that demonstrate better performance to ensure the improvement of ASR indices in order to offer lower restoration time with improved system reliability.

Acknowledgement

The authors wish to thank the authorities of Annamalai University, Annamalainagar, Tamilnadu, India for the facilities provided to prepare this paper.

Nomenclatures

K_{Di}	Derivative feedback gain of area *i*
K_{Di}	Derivative feedback gain of area *i*
K_{HES}	Gain constant of Hydrogen Energy Storage
K_{HES}	Gain constant of Hydrogen Energy Storage
K_{Ii}	Integral feedback gain of area *i*
K_{Ii}	Integral feedback gain of area *i*
K_{pi}	Gain associated with the transfer function of the area, Hz / p.u. MW
K_{Pi}	Proportional feedback gain of area *i*
K_{pi}	Gain associated with the transfer function of the area, Hz / p.u. MW
K_{Pi}	Proportional feedback gain of area *i*
N	Number of interconnected areas
N	Number of interconnected areas
P_{Ci}	Area speed changer output, p.u.MW
P_{Ci}	Area speed changer output, p.u.MW
P_{Di}	Area real power load, p.u.MW
P_{Di}	Area real power load, p.u.MW
Pei	The total power exchange of area-i, p.u.MW/Hz
P_{Mi}	Mechanical (turbine) power output, p.u.MW
P_{Mi}	Mechanical (turbine) power output, p.u.MW
R	Steady state regulation of the governor, Hz/ p.u. MW
T_g	Steam turbine speed governor time constant, s
T_{HES}	Time constant of the Hydrogen Energy Storage, s
T_{IPFC}	Time constant of the Interline Power Flow Controller, s
T_{ps}	Area time constant, sec

Abbreviations

AGC	Automatic Generation Control
ASR	Ancillary Service Requirement
BBBC	Big Bang Big Crunch
DISCO	Distribution companies
DPM	Disco Participation Matrix
FACTS	Flexible Alternative Current Transmission System
FPA	Flower Pollination Algorithm
GENCO	Generation companies
HES	Hydrogen Energy Storage
IPFC	Interline Power Flow Controller
PIDF	Proportional Integral Derivative with Filter controller

References

1. Rahi, O.P.; Thakur, H.K.; Singh, A.K.; and Gupta, S.K. (2013). Ancillary services in restructured environment of power system. *International Journal of Innovative Technology and Research*, 1(3), 218-225.
2. Pappachen, A.; and Fathima, A.P. (2017). Critical research areas on load frequency control issues in a deregulated power system: A state-of-the-art-of-review. *Renewable and Sustainable Energy Reviews*, 72, 163-177.
3. Kundur, p. (2009). *Power system stability and control*. (8th reprint). Tata McGraw-Hill.
4. Shankar, R.; Pradhan, S.R.; Chatterjee, K.; and Mandal, R. (2017). A comprehensive state of the art literature survey on LFC mechanism for power system. *Renewable and Sustainable Energy Reviews*, 76, 1185-1207.
5. Donde, V.; Pai, M.A.; and Hiskens, I.A. (2001). Simulation and optimization in an AGC system after deregulation. *IEEE Transactions on Power systems*, 16(3), 481-489.
6. Nain, P.; Parmar, K.S; and Singh, A.K. (2013). Automatic generation control of an interconnected power system before and after deregulation. *International Journal of Computer Applications*, 61(15), 11-16.
7. Sharma, P. (2014). AGC strategies-A review. *International Journal of Engineering Research*, 2(4), 68-77.
8. Saikia, L.C.; Nanda,; and Mishra, S. (2011). Performance comparison of several classical controllers in AGC for multi-area interconnected thermal system. *International Journal of Electrical Power & Energy Systems*, 33(3), 394-401.
9. Shabani, H.; Vahidi, B.; and Ebrahimpour, M. (2013). A robust PID controller based on imperialist competitive algorithm for load-frequency control of power systems. *ISA transactions*, 52(1), 88-95.
10. Singh Parmar, K.S.; Majhi, S.; and Kothari, D.P. (2014). LFC of an interconnected power system with multi-source power generation in deregulated power environment. *International Journal of Electrical Power & Energy Systems*, 57, 277-286.
11. Sahu, R.K.; Panda, S.; and Padhan, S. (2014). Optimal gravitational search algorithm for automatic generation control of interconnected power systems. *Ain Shams Engineering Journal*, 5(3), 721-733.

12. Shayeghi, H.A.; Shayanfar, H.A.; and Jalili, A. (2009). Load frequency control strategies: A state-of-the-art survey for the researcher. *Energy Conversion and management*, 50(2), 344-353.
13. Erol, O.K.; and Eksin, I. (2006). A new optimization method: big bang–big crunch. *Advances in Engineering Software*, 37(2), 106-111.
14. Kumar, N.; Kumar, V.; and Tyagi, B., (2016). Optimization of PID parameters using BBBC for a multiarea AGC scheme in a deregulated power system. *Turkish Journal of Electrical Engineering & Computer Sciences*, 24(5), 4105-4116.
15. Shankar, R.; Chatterjee, K.; and Bhushan, R. (2016). Impact of energy storage system on load frequency control for diverse sources of interconnected power system in deregulated power environment. *International Journal of Electrical Power & Energy Systems*, 79, 11-26.
16. Chatterjee, K. (2011). Effect of battery energy storage system on load frequency control under deregulation. *International Journal of Emerging Electric Power Systems*, 12(3), 12-17.
17. Hingorani, N.G.; Gyugyi, L.; and El-Hawary, M. (2000). *Understanding FACTS: concepts and technology of flexible AC transmission systems*, New York: IEEE press.
18. Chidambaram, I.A.; and Paramasivam, B. (2013). Optimized load-frequency simulation in restructured power system with redox flow batteries and interline power flow controller. *International Journal of Electrical Power & Energy Systems*, 50, 9-24.
19. Gorripotu, T.S.; Sahu, R.K.; and Panda, S. (2015). AGC of a multi-area power system under deregulated environment using redox flow batteries and interline power flow controller. *Engineering Science and Technology, an International Journal*, 18(4), 555-578.
20. Ipsakis, D.; Voutetakis, S.; Seferlis, P.; Stergiopoulos, F.; and Elmasides, C. (2009). Power management strategies for a stand-alone power system using renewable energy sources and hydrogen storage. *International journal of hydrogen energy*, 34(16), 7081-7095.
21. Pathak, N.; Verma, A.; and Bhatti, T.S. (2016). Automatic generation control of thermal power system under varying steam turbine dynamic model parameters based on generation schedules of the plants. *The Journal of Engineering*, 1(1), 1-13.
22. Ibrahim, El-Henawy.; Nagham Ahmed,; and Abdelmegeed. (2018). Meta-heuristics algorithms: A survey. *International Journal of Computer Applications*, 179(22), 45-54.
23. Jiang, S.; Gole, A.M.; Annakkage, U.D.; and Jacobson, D.A. (2011). Damping performance analysis of IPFC and UPFC controllers using validated small-signal models. *IEEE Transactions on Power Delivery*, 26(1), 446-454.

Appendix – A

Table A-1. Control area and Gencos parameters (thermal generating unit) and parameter of HES and IPFC unit [18, 20]

Parameters	**Area1**	**Area 2**
Area capacities	1000 MW	1000 MW
Rating of single generating machine	500 MW	500 MW
***Kp* (Hz/p.u.MW)**	120	120
***Tp* (s)**	20	20
***B* (p.u.MW / Hz)**	0.425	0.425
***R* (Hz / p.u.MW)**	$R_1 = R_2 = 2.4$	$R_3 = R_4 = 2.4$
***Tg* (s)**	$T_{g1} = T_{g2} = 0.08$	$T_{g3} = T_{g4} = 0.08$
Synchronising coefficient (p.u.MW / Hz)	$2\pi T_{12} = 0.545$	
System frequency (F) in Hz	60 Hz	
Area participation factor (apf)	$apf_{11} = apf_{12} = apf_{21} = apf_{22} = 0.5$	
Area capacity ratios	$a_{12} = -1$	
Time constant of HES unit	$T_{HES} = 0.04$ sec	
Time constant of IPFC unit	$T_{IPFC} = 0.01$ sec	

Table A-2. Steam turbine data at different generation schedules [21].

Generation schedules, %	**Time constants in sec**			**Power fractions of HP.IP and LP turbines**		
	T_{SC}	T_{RH}	T_{CO}	F_{HP}	F_{IP}	F_{LP}
100	0.2990	5.00	0.4000	0.2727	0.3511	0.3760
80	0.3746	5.01	0.3970	0.2719	0.3560	0.3720
60	0.4922	5.02	0.3966	0.2728	0.3647	0.3623
50	0.5786	5.04	0.3932	0.2872	0.3790	0.3338
30	0.8947	5.37	0.4248	0.3299	0.3828	0.2872